

Impact of unidentified light charged hadron data on the determination of pion fragmentation functions

Maryam Soleymaninia^{1,3,*}, Muhammad Goharipour^{3,†}, and Hamzeh Khanpour^{2,3‡}

¹*Institute of Advanced Technologies, Shahid Rajaee*

Teacher Training University, Lavizan, Tehran, 16788, Iran

²*Department of Physics, University of Science and Technology
of Mazandaran, P.O.Box 48518-78195, Behshahr, Iran*

³*School of Particles and Accelerators, Institute for Research in
Fundamental Sciences (IPM), P.O.Box 19395-5531, Tehran, Iran*

In this paper a new comprehensive analysis of parton-to-pion fragmentation functions (FFs) is performed for the first time by including all experimental data sets on single inclusive pion as well as unidentified light charged hadron production in electron-positron (e^+e^-) annihilation. We determine the pion FFs along with their uncertainties using the standard “Hessian” technique at next-to-leading order (NLO) and next-to-next-to leading order (NNLO) in perturbative QCD. It is shown that the determination of pion FFs using simultaneously the data sets from pion and unidentified light charged hadron productions leads to the reduction of all pion FFs uncertainties especially for the case of strange quark and gluon FFs by significant factors. In this study, we have quantified the constraints that these data sets could impose on the extracted pion FFs. Our results also illustrate the significant improvement in the precision of FFs fits achievable by inclusion of higher order corrections. The improvements on both FFs uncertainties as well as fit quality have been clearly discussed.

PACS numbers: 11.30.Hv, 14.65.Bt, 12.38.Lg

* Maryam_Soleymaninia@ipm.ir

† [Muhammad.Goharipour@ipm.ir](mailto:Mohammad.Goharipour@ipm.ir)

‡ Hamzeh.Khanpour@mail.ipm.ir

CONTENTS

I. Introduction	2
II. Experimental data selection	5
III. Theoretical methodology for calculations and fitting	7
IV. Analysis results	12
A. Comparison of χ^2 values	13
B. Comparison of the relative uncertainties	15
C. Comparison of the “pion+hadron fit” at NLO and NNLO accuracy	25
D. Comparison of the data and theory predictions	25
V. Summary and Conclusions	27
Acknowledgments	29
References	29

I. INTRODUCTION

Essential ingredients of theoretical predictions for the present or future hadron colliders such as the large hadron collider (LHC) and large hadron-electron collider (LHeC), are the detailed understanding of the quark and gluon structure of the nucleon [1–4]. These are quantified by the parton distribution functions (PDFs) [5–7] as well as the fragmentation functions (FFs) [8–20]. In recent years, precise determination of PDFs as well as FFs including their experimental uncertainties had become an active topic for many LHC processes, including top-quark and Higgs boson sector, searches for new heavy beyond the Standard Model (BSM) particles, searches for new physics (NP) as well as in the measurement of fundamental SM parameters such as the strong coupling constant. For

more details, we refer the readers to the literature [21–23] and a recent study on the PDFs at the High-Luminosity LHC (HL-LHC) [1].

In a hard-scattering collision, PDFs determine how the proton’s momentum is shared among its constituents. Likewise, the FFs describe the probability density for the fragmentation of the final-state parton with a certain momentum into the hadron with a fraction of the parton’s momentum. PDFs and the FFs depend on the factorization scale. This dependence is described by the DGLAP evolution equations [24–27], which allow the calculation of the PDFs and FFs, if they are known at a given initial scale, i.e. $\mu^2 = \mu_0^2$. It is well known that the PDFs and the FFs can not be calculable in perturbation theory, and hence, these distributions need to be extracted from experimental information through a QCD fit. In addition, these non-perturbative functions are also universal. The universality of PDFs and FFs commonly refers that, since the hadronization processes are not sensitive to the particular choices of hard scattering process in short range, these non-perturbative functions can be extracted from certain kind of scattering experimental observables. Then the extracted distributions can be used for the theory predictions of scattering observable in high energy collisions.

The new and precise data sets are vital for the precise determination of FFs. These data sets have been and currently been collected from different high energy processes at variety of lepton and hadron colliders. These processes include the hadron production data in single-inclusive electron-positron (e^+e^-) annihilation (SIA), semi-inclusive deep inelastic scattering (SIDIS), and proton-proton and proton-antiproton collisions measured by TEVATRON, RHIC and LHC. For a list of all available data sets, we refer the readers to the recent analysis by NNPDF collaboration and references therein [8, 9]. Several analyses have been done so far to extract FFs using the observables mentioned above. Among them are the recent determination of charged hadron FFs from collider data by NNPDF collaboration, NNFF1.1h [8]. This collaboration also have determined the pions, kaons, and proton FFs using the SIA data sets at NNLO in perturbative QCD based on the NNPDF

methodology, NNFF1.0 [9]. The recent analyses by HKKS16 [13] and JAM16 [28] also have been performed using the SIA data only. Other analyses in literature can be found for example in Refs. [29–36]

Recently, we also have performed the First determination of $D^{*\pm}$ -meson FFs and their uncertainties at NNLO, SKM18 [10]. In Ref. [11] we presented our QCD analysis of charged hadron FFs and their uncertainties at NLO and NNLO (SGK18) which is the first determination of light charged hadron FFs at NNLO accuracy. Finally in Ref. [12] the contributions from *residual* light charged hadrons in the inclusive charged hadrons have been extracted using the e^+e^- annihilation data sets. Since the QCD framework for FFs at NNLO are not accessible for SIDIS, and hadron-hadron collisions, both of our analyses are restricted to the single-inclusive charged hadron production in electron-positron annihilation. The uncertainties in our recent analyses on FFs as well as the corresponding observables are estimated using the “Hessian” technique.

In this work, an extraction of pion FFs from QCD analysis of electron-positron annihilation experimental data in zero-mass variable flavor number scheme (ZM-VFNS) has been presented. The main aim of this paper is to examine, for the first time, the impact of unidentified light charged hadron experimental data on the determination of pion FFs and their uncertainties at NLO and NNLO accuracy. In this respect, we have attempted a determination of pion FFs considering two different scenarios. First, we present a determination of pion FFs through a QCD analysis of pion data sets. In this first study of FFs, which is performed within ZM-VFNS at both NLO and NNLO approximations and referred to as “pion fit”, we simplify the analysis by considering the pion data sets only. Secondly, we determine pion FFs through a QCD analysis by including both pion and unidentified light charged hadron data sets. We show that the fitting simultaneously the pion FFs using both data sets leads to a well-constrained determination of pion FFs including significant effect on the extracted uncertainties. Our second fit entitled as “pion+hadron fit”.

The outline of this paper is as follows. In section II, we present in details all available

SIA data sets for pion production as well as the SIA data sets for the unidentified light charged hadrons. In Section III, we discuss the theoretical formalism of single-hadron inclusive production in electron-positron (e^+e^-) annihilation. This section also includes the detailed discussions of our fitting process and parameterization for the pion FFs. Section IV is then dedicated to our results. The obtained results are clearly discussed for variety of aspect in this section, and comparison with other analyses in literature also presented. This section also includes our theory predictions based on the extracted pion FFs including a comparison with all data analyzed. Finally, Section V includes a summary and our conclusions.

II. EXPERIMENTAL DATA SELECTION

In this section, we present the experimental data sets that are included in our “pion fit” and “pion+hadron fit” analyses. As we mentioned in the Introduction, our QCD fits are performed by inducing the electron-positron annihilation data in two scenarios: In the first analysis, we use the available SIA data for pion from Refs. [37–46] to extract the pion FFs. In the second analysis, the SIA data sets for the unidentified charged hadrons [41, 44, 46–51] along with the pion data sets are included in our fits to calculate the FFs of pion. All the data sets for pion and unidentified hadrons are listed in Tables I and II for inclusive and flavor-tagged SIA data which are reported by different experiments. Note that, the measured observables for these data sets, specially for pion, are different and a complete explanation about SIA pion data and the relations between the scaling variables are available in related analysis done by NNPDF collaboration in NNFF1.0 [9]. In addition, we have used the unidentified light charged hadron experimental data in our recent study of (SGK18) [11]. The details of corrections to these data sets and the kinematic cuts applied are presented in Ref. [11].

According to the data sets presented in second column of Tables I and II, the observables are different and provide limited sensitivity to the separation between light and

heavy quark FFs due to the flavor-tagged data. Since the gluon receives its leading order (LO) accuracy at $\mathcal{O}(\alpha_f)$, the total SIA cross sections are poor to constrain this density. However, the longitudinal cross sections can impose a comparable sensitivity to the gluon FF because the longitudinal coefficient functions start at $\mathcal{O}(\alpha_f)$. Hence, the longitudinal observables that are available for the unidentified hadrons could constrain the gluon FF well enough. It should be noted that the NNLO QCD corrections for longitudinal structure functions are not available in the literature, and hence, such corrections can not be considered in our analyses.

In this paper, we plan to study the effects arising from the unidentified light charged hadron experimental data on the calculation of pion FFs by including both pion and unidentified hadron data sets, and then, compare the extracted pion FFs with the results calculated from the QCD analysis using pion data sets alone. Since the most contribution of FFs into the unidentified light charged hadron cross sections mainly comes from the identified pion FFs, it motivates us to investigate the effect of unidentified light charged hadron data sets on the reduction of pion FFs uncertainties. In Tables. I and II, our results are reported at NLO and NNLO accuracies of perturbative QCD. In both tables, the fourth column presents our fit results for the value of χ^2 per number of data points ($\chi^2/N_{pts.}$) considering pion data sets in the fit, while in the fifth column the same quantity are reported considering the pion and light hadron experimental data sets in the analysis. One of the most important findings from these tables are the significant reduction of χ^2/dof by going from NLO to the NNLO corrections. We will return to this issue in the next section.

In order to avoid the sensitivity of behaviors of FF parametrization in the low and high regions of z , we apply cuts on the momentum fraction z . We exactly follow the cuts applied in our recent study on light charged hadron FFs, SGK18 [11]. These selections are also imposed for the pion experimental data. For data sets at $\sqrt{s} = M_Z$, we include the data points with the scaling variable of $z \geq 0.02$ and for $\sqrt{s} < M_Z$, the data points with

$z \geq 0.075$ are included in our QCD fits. The data points with $z > 0.9$ are excluded in all of our QCD analyses. Considering the kinematical cut applied, the number of the data points are listed separately in the denominator of the forth and fifth columns in Tables. [I](#) and [II](#) for the NLO and NNLO accuracy, respectively.

III. THEORETICAL METHODOLOGY FOR CALCULATIONS AND FITTING

In this section, a brief review of the theoretical framework and our methodology has been presented. According to the factorization theorem, the SIA differential cross section normalized to the total cross section $\frac{1}{\sigma_{\text{tot}}} \frac{d\sigma^{H^\pm}}{dz}$ at a given center-of-mass energy of $\sqrt{s} = Q$ is written by,

$$\frac{1}{\sigma_{\text{tot}}} \frac{d\sigma^{H^\pm}}{dz} = \frac{1}{\sigma_{\text{tot}}} \left[F_T^{H^\pm}(z, Q) + F_L^{H^\pm}(z, Q) \right]. \quad (1)$$

This equation is used for identified charged hadrons such as π^\pm , K^\pm and p/\bar{p} and, unidentified hadrons h^\pm . In Eq. (1), H^\pm is defined as sum of different charge of hadrons $H = H^+ + H^-$ and $z = \frac{2E_H}{\sqrt{s}}$ is the scaling variable. The total cross section σ_{tot} depends to the perturbative order of QCD corrections and detail explanations can be found, for example, in Ref. [\[11\]](#). According to the Eq. (1), in the case of multiplicities, the differential cross section for SIA processes can be decomposed into time-like structure functions F_T and F_L which are the transverse (T) and longitudinal (L) perturbative parts, respectively. The time-like structure functions can be written as convolutions of a perturbative part, coefficient functions $C_i(z, \alpha_s)$, and a nonperturbative part, FFs $D^{H^\pm}(z, Q)$,

$$F^{H^\pm}(z, Q) = \sum_i C_i(z, \alpha_s) \otimes D^{H^\pm}(z, Q). \quad (2)$$

The coefficient functions have been calculated in Refs. [\[52–54\]](#) and they are available up to NNLO accuracy for electron positron annihilations. It should be mentioned here that, in this analysis, the renormalization scale μ_R and the factorization scale μ_F considered to be equal to the center-of-mass energy of collision, $\mu_R = \mu_F = \sqrt{s}$.

Dataset	observable	\sqrt{s} [GeV]	$\chi^2/pts.$ "pion"	$\chi^2/pts.$ "pion+hadron"
BELLE [37]	inclusive	10.52	38.37/70	42.28/70
BABAR [38]	inclusive	10.54	78.07/40	81.64/40
TASSO12 [39]	inclusive	12	4.24/4	4.05/4
TASSO14 [40]	inclusive	14	11.76/9	12.04/9
TASSO22 [40]	inclusive	22	25.39/8	26.55/8
TPC [41]	inclusive	29	7.05/13	8.25/13
TASSO34 [42]	inclusive	34	19.22/9	23.26/9
TASSO44 [42]	inclusive	44	18.21/6	19.95/6
ALEPH [43]	inclusive	91.2	37.77/23	43.07/23
DELPHI [44]	inclusive	91.2	27.52/21	22.86/21
	<i>uds</i> tag	91.2	21.47/21	22.70/21
	<i>b</i> tag	91.2	21.12/21	11.11/21
OPAL [45]	inclusive	91.2	32.01/24	37.41 /24
SLD [46]	inclusive	91.2	57.87/34	76.20/34
	<i>uds</i> tag	91.2	90.98/34	92.04/34
	<i>c</i> tag	91.2	38.83/34	40.13/34
	<i>b</i> tag	91.2	19.81/34	38.28/34
TASSO14 [47]	inclusive	14	—	8.22/15
TASSO22 [47]	inclusive	22	—	13.07/15
TPC [41]	inclusive	29	—	20.72/21
TASSO35 [47]	inclusive	34	—	21.74/15
TASSO44 [47]	inclusive	44	—	18.80/15
ALEPH [48]	inclusive	91.2	—	9.23/32
DELPHI [44, 49]	inclusive	91.2	—	16.86/22
	<i>uds</i> tag	91.2	—	10.52/22
	<i>b</i> tag	91.2	—	51.76/22
	Longitudinal inclusive	91.2	—	28.49/20
	Longitudinal <i>b</i> tag	91.2	—	20.12/20
OPAL [50, 51]	inclusive	91.2	—	12.40/20
	<i>uds</i> tag	91.2	—	7.34/20
	<i>c</i> tag	91.2	—	14.18/20
	<i>b</i> tag	91.2	—	26.85/20
	Longitudinal inclusive	91.2	—	89.18/20
SLD [46]	inclusive	91.2	—	15.09/34
	<i>uds</i> tag	91.2	—	15.86/34
	<i>c</i> tag	91.2	—	29.26/34
	<i>b</i> tag	91.2	—	81.21/34
Total χ^2/dof			1.42	1.44

TABLE I. The data sets included in the analyses of π^\pm FFs at NLO. For each experiment, we indicate the corresponding reference, the measured observables, the center-of-mass energy \sqrt{s} , the $\chi^2/pts.$ values for every data set, as well as the total χ^2/dof .

Dataset	observable	\sqrt{s} [GeV]	$\chi^2/\text{pts. "pion"}$	$\chi^2/\text{pts. "pion+hadron"}$
BELLE [37]	inclusive	10.52	27.39/70	29.96/70
BABAR [38]	inclusive	10.54	59.84/40	57.80/40
TASSO12 [39]	inclusive	12	4.28/4	4.21/4
TASSO14 [40]	inclusive	14	11.50/9	11.67/9
TASSO22 [40]	inclusive	22	23.17/8	24.09/8
TPC [41]	inclusive	29	10.07/13	9.26/13
TASSO34 [42]	inclusive	34	14.44/9	15.93/9
TASSO44 [42]	inclusive	44	16.93/6	17.78/6
ALEPH [43]	inclusive	91.2	27.63/23	35.50/23
DELPHI [44]	inclusive	91.2	29.79/21	24.78/21
	<i>uds</i> tag	91.2	22.22/21	23.57/21
	<i>b</i> tag	91.2	19.96/21	10.57/21
OPAL [45]	inclusive	91.2	30.53/24	35.74 /24
SLD [46]	inclusive	91.2	37.60/34	47.80/34
	<i>uds</i> tag	91.2	68.97/34	66.70/34
	<i>c</i> tag	91.2	31.73/34	35.18/34
	<i>b</i> tag	91.2	19.36/34	40.38/34
TASSO14 [47]	inclusive	14	—	8.78/15
TASSO22 [47]	inclusive	22	—	13.22/15
TPC [41]	inclusive	29	—	15.69/21
TASSO35 [47]	inclusive	34	—	23.33/15
TASSO44 [47]	inclusive	44	—	19.41/15
ALEPH [48]	inclusive	91.2	—	10.62/32
DELPHI [44, 49]	inclusive	91.2	—	18.55/22
	<i>uds</i> tag	91.2	—	11.66/22
	<i>b</i> tag	91.2	—	50.99/22
	Longitudinal inclusive	91.2	—	9.47/20
	Longitudinal <i>b</i> tag	91.2	—	9.37/20
OPAL [50, 51]	inclusive	91.2	—	14.23/20
	<i>uds</i> tag	91.2	—	8.53/20
	<i>c</i> tag	91.2	—	14.56/20
	<i>b</i> tag	91.2	—	26.41/20
	Longitudinal inclusive	91.2	—	7.99/20
SLD [46]	inclusive	91.2	—	10.31/34
	<i>uds</i> tag	91.2	—	10.97/34
	<i>c</i> tag	91.2	—	29.74/34
	<i>b</i> tag	91.2	—	80.62/34
Total χ^2/dof			1.17	1.06

TABLE II. Same as Table. I but at NNLO accuracy.

Since the universal FFs are nonperturbative functions, in order to determine the FFs, one needs to parametrize the functions of partons $i = q, \bar{q}, g$ at a given initial scale. The z parameter represents the fraction of the parton momentum which carried by hadron. Theoretically, the renormalization equations govern the scale dependence of the FFs and they can be evaluate to a given higher energy scale using the DGLAP evolution equations. In our analysis, we use the publicly APFEL package [55] in order to calculate of the SIA cross sections as well as the evolution of FFs by DGLAP equations up to NNLO accuracy. In addition, the ZM-VFNS is considered to account the heavy quarks contributions, and hence, the effects of heavy quark mass are not taken into account in our analysis.

Our main aim in this analysis is to study the effect of adding all the unidentified light charged hadrons experimental data to the pion ones from SIA processes in the procedure of determination of pion FFs. Hence, we need the theoretical definition of unidentified charge hadron FFs in our calculations. Experimentally, the unidentified light charged hadrons contain all identified light hadrons such as pion, kaon, proton and a small *residual* light hadrons. Then unidentified charged hadron cross sections of SIA can be calculated by summing of individual cross sections of the identified light ones (π^\pm, K^\pm and p/\bar{p}) and the *residual* contribution. The SIA coefficient functions for all final states are the same, and hence, the FFs of unidentified light charged hadrons (D^{h^\pm}) can be defined as the sum of the pion, kaon and proton FFs ($D^{\pi^\pm}, D^{K^\pm}, D^{p/\bar{p}}$) including the *residual* light hadron FFs D^{res^\pm}

$$D^{h^\pm} = D^{\pi^\pm} + D^{K^\pm} + D^{p/\bar{p}} + D^{res^\pm}. \quad (3)$$

Since our aim in this analysis is a new determination of pion FFs D^{π^\pm} , we use the kaon and proton FFs from NNFF1.0 parton set [9] both at NLO and NNLO accuracies. Recently, we have calculated the *residual* light hadron FFs D^{res^\pm} in Ref. [12] up to NNLO QCD correction. In Ref. [12], we have shown that the contribution of the *residual* light hadrons are small, and hence, one can ignore this small contribution in Eq. (3). The contribution from this small distribution are not significant for the case of total or light charged cross sections, however, for the case of c - and b -tagged cross sections they are sizable.

For the uncertainty from NNFF1.0, we follow the analysis by DSS07 in Ref. [36] and estimate an average uncertainty of 5% in all theoretical calculations of the inclusive charged hadron cross sections stemming from the large uncertainties of kaon and proton FFs from NNFF1.0 set. In addition, our recent study shows that an additional uncertainty due to the contributions of *residual* charged hadrons FFs [12] also need to be taken into account. Overall, we believe that a 8% of the cross section value seems to be reasonable. These additional uncertainties are included in the χ^2 minimization procedure for determining the pion FFs. In order to add these uncertainties, we apply such a simplest way to include a “theory” error which we add it in quadrature to the statistical and systematic experimental error in the χ^2 expression. This is the standard approach that one can use to add this additional uncertainty to the QCD analysis. The method of the present study are also consistent with those of DSS07 [36] who used the same approach, and hence, our results share a number of similarities with DSS07 findings. This method was chosen because it is one of the most practical and economic ways to include such uncertainty and in agreement from previous results reported in the literature. However this method may suffers from a number of pitfalls. One need to use a rigorous approach and include the full NNFF1.0 uncertainties in the kaon and proton FFs in Eq. (3). In order to ensure the affect of this alternative method on our conclusions, we also examined this approach. Our study shows that one can reaches the same conclusions, finding no increase in the size of uncertainty. For the physical parameters, we exactly follow the analysis by NNFF collaboration, NNFF1.0. We use the heavy flavor masses for charm and bottom as $m_c = 1.51$ GeV and $m_b = 4.92$ GeV [8, 9], respectively. Also the Z-boson mass is chosen to be $M_Z = 91.187$ GeV and the QCD coupling constant is fixed to the world average $\alpha_s(M_Z) = 0.1185$ [56].

Now we are in a position to present our QCD fit methodology, input functional form as well as the assumptions we used in our analysis to determine the pion FFs. We choose a flexible input parametrization for pion FFs at initial scale Q_0 which we also used in our

very recent analysis of unidentified light charged hadrons [11],

$$D_i^{\pi^\pm}(z, Q_0) = \frac{\mathcal{N}_i z^{\alpha_i} (1-z)^{\beta_i} [1 + \gamma_i (1-z)^{\delta_i}]}{B[2 + \alpha_i, \beta_i + 1] + \gamma_i B[2 + \alpha_i, \beta_i + \delta_i + 1]}, \quad (4)$$

where $i = u^+, d^+, s^+, c^+, b^+$ and $g, q^+ = q + \bar{q}$. In order to normalize the parameter \mathcal{N}_i we use the Euler Beta function $B[a, b]$. Since we include the FF sets of NNFF1.0 for kaon and proton, we choose the initial scale of energy $Q_0 = 5 \text{ GeV}$ and therefore the number of active flavors in our analyses need to be fixed at $n_f = 5$. In addition, the charge conjugation and isospin symmetry $D_{u^+}^{\pi^\pm} = D_{d^+}^{\pi^\pm}$ are assumed. More specifically, the γ and δ parameters for s^+, c^+ and g could not well constrain by the SIA data and we are forced to fix them as $\gamma_{s^+, c^+, g} = 0$ and $\delta_{s^+, c^+, g} = 0$. Then the best fit is only achieved with all five parameters of Eq. (4) for u^+ and b^+ . We determine 19 free parameters by a standard χ^2 minimization strategy in which the details can be found in Refs. [11, 57].

The free parameters are determined from the best fit, and we list them in Table. III. In the second and third columns of this table, we report our best fit parameters for only pion data analysis at NLO and NNLO accuracy, respectively. The parameters reported by the forth and fifth columns are for the analyses with both pion and unidentified hadron data sets at both perturbative orders.

IV. ANALYSIS RESULTS

After the detailed presenting of the experimental data sets included in the present work and the theoretical and phenomenological framework of the analysis in the previous sections, in the following we present the numerical results obtained for the pion FFs from different analyses and compare them with each other. As we mentioned before, the main goal of the present work is to investigate, for the first time, the impact of unidentified light charged hadron experimental data on the pion FFs at both NLO and NNLO accuracy. In this respect, the pion FFs should be determined by performing two different analyses: 1)

determination of pion FFs through a QCD analysis of only pion data sets as usual (*pion fit*), and 2) determination of pion FFs through a simultaneous analysis of both pion and unidentified light charged hadron data sets (*pion+hadron fit*).

The important point that should be noted is the presence of the kaon, proton and *residual* FFs in the theoretical calculation of the unidentified light charged hadron cross sections which is required for the second analysis. As discussed in Sec. III, we use the kaon and proton FFs from the NNFF1.0 analysis [9] and ignore the small *residual* contribution. Hence, some theoretical uncertainties should be taken into account in the analysis containing the unidentified light charged hadron data. One of the most common methods is adding a point-to-point uncertainty to the experimental data as a systematic error source, 8% in our analyses.

A. Comparison of χ^2 values

The list of experimental data sets including their references as well as the results of our analyses introduced above have been summarized in Tables I and II at NLO and NNLO, respectively. In each table, the second column indicates the kind of observable measured by each experiment and the third column specifies its related value of center-of-mass energy. Note also that the columns labeled by “*pion*” and “*pion+hadron*” are containing the results of the first and second analyses, respectively. The values of χ^2 per number of data points ($\chi^2/N_{\text{pts.}}$) have been presented in these columns for each data set. Moreover, the value of total χ^2 divide by the number of degrees of freedom (χ^2/dof) for each analysis is presented in the last row of the table. The total number of data points included in the “*pion fit*” analysis is 405, while it is 879 for the “*pion+hadron fit*” analysis. According to the results obtained, the following conclusions can be drawn. For the case of NLO analyses, although the values of $\chi^2/N_{\text{pts.}}$ have increased almost for each pion data set after the inclusion of the unidentified light charged hadron data, but the values of χ^2/dof for the “*pion fit*” and “*pion+hadron fit*” analyses are almost equal. Such behavior is seen

Parameter	“pion” NLO	“pion” NNLO	“pion+hadron” NLO	“pion+hadron” NNLO
\mathcal{N}_{u^+}	1.123	1.062	1.133	1.071
α_{u^+}	-0.617	-0.713	-0.558	-0.671
β_{u^+}	1.737	1.854	1.757	1.862
γ_{u^+}	8.324	6.550	9.705	7.742
δ_{u^+}	5.175	5.843	5.314	6.163
\mathcal{N}_{s^+}	0.239	0.456	0.124	0.397
α_{s^+}	1.634	0.598	3.376	0.986
β_{s^+}	10.714	8.468	12.658	8.873
\mathcal{N}_{c^+}	0.739	0.777	0.724	0.773
α_{c^+}	-0.903	-0.901	-0.929	-0.907
β_{c^+}	4.662	5.055	4.520	4.917
\mathcal{N}_{b^+}	0.694	0.735	0.673	0.735
α_{b^+}	-0.395	-0.446	-0.346	-0.449
β_{b^+}	5.346	5.057	4.728	4.500
γ_{b^+}	6.014	7.356	9.098	8.735
δ_{b^+}	9.102	8.567	10.573	9.086
\mathcal{N}_g	0.616	0.571	0.705	0.611
α_g	0.406	0.137	-0.230	-0.068
β_g	14.210	16.174	8.658	13.688

TABLE III. The best fit parameters for the fragmentation of partons into the π^\pm for both pion fit and pion+hadron fit analyses at NLO and NNLO accuracy. The starting scale is taken to be $Q_0 = 5$ GeV for all parton species.

for some of the data sets in the case of NNLO analyses, but with the difference that the value of χ^2/dof has decreased by including the unidentified light charged hadron data in the analysis. Another point should be noted here is the significant reduction in the value of χ^2/dof when we move from NLO to NNLO. The optimum values of fit parameters have been presented in Table. III, where the first and second columns are related to the pion data analyses at NLO and NNLO, respectively, while the third and fourth columns contain the results of the simultaneous analyses of the pion and hadron data at NLO and NNLO accuracy.

B. Comparison of the relative uncertainties

In order to investigate the impact arising from the inclusion of unidentified light charged hadron experimental data on pion FFs both in behavior and uncertainty, the results obtained from “pion fit” and “pion+hadron fit” can be compared in various ways. One of the best approaches to check the validity and excellency of the new results obtained, specifically in view of the uncertainties, is comparing the relative uncertainties of the extracted distributions which are obtained, for each analysis separately, by dividing the upper and lower bands to the central values. Fig. 1 shows a comparison between the relative uncertainties of pion FFs obtained from the “pion fit” and “pion+hadron fit” analyses at NLO accuracy. We have presented the results for all flavors parameterized in the analysis at the initial scale of $Q_0 = 5$ GeV. As can be seen, except for the case of $s + \bar{s}$ FF, the relative uncertainties of pion FFs obtained from the simultaneous analysis of the pion and hadron data are smaller than those obtained by fitting the pion data alone, especially for the case of gluon FF. In fact, the amount of the uncertainty of $s + \bar{s}$ FF from “pion+hadron fit” analysis is also less than “pion fit” analysis (as will be shown later), but since its central value is smaller by a factor of two, it has overall a relative uncertainty which is somewhat larger.

Fig. 2 shows the same results as Fig. 1, but this time for our NNLO analysis. One can clearly conclude that the inclusion of the unidentified light charged hadron data in the pion FFs analysis at NNLO accuracy can also lead to a smaller relative uncertainty for all flavors. Note that, compared with the NLO results, the relative uncertainty of $s + \bar{s}$ FF from “pion+hadron fit” analysis has now remarkably decreased at lower z values rather than its distribution from “pion fit” analysis. Overall, the results obtained indicate that by performing a simultaneous analysis of pion and unidentified light charged hadron data, a pion FFs set with more acceptable uncertainties can be obtained at both NLO and NNLO accuracies.

To study the effects of the evolution and also evaluate the results at a given higher

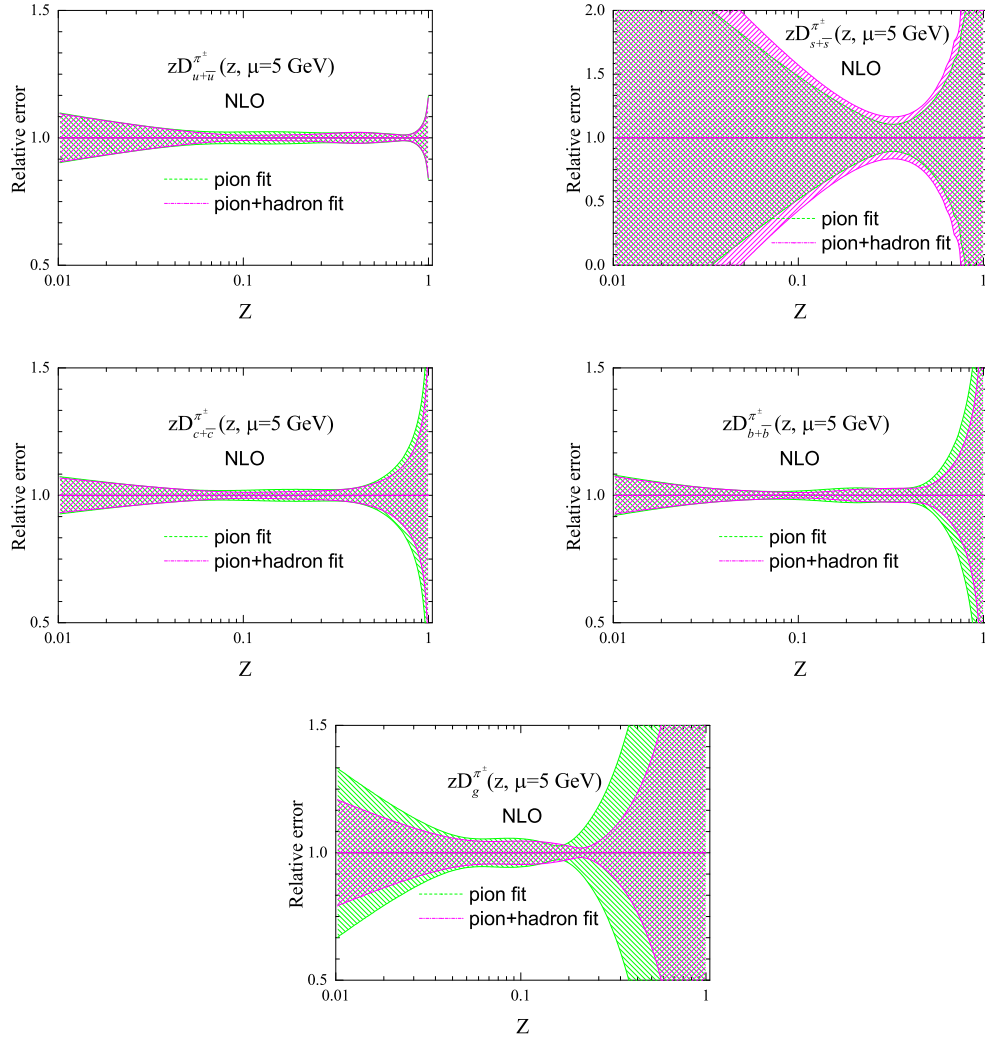


FIG. 1. Comparison between the relative uncertainties of pion FFs at $Q_0 = 5 \text{ GeV}$ obtained from the “pion fit” and “pion+hadron fit” analyses at NLO.

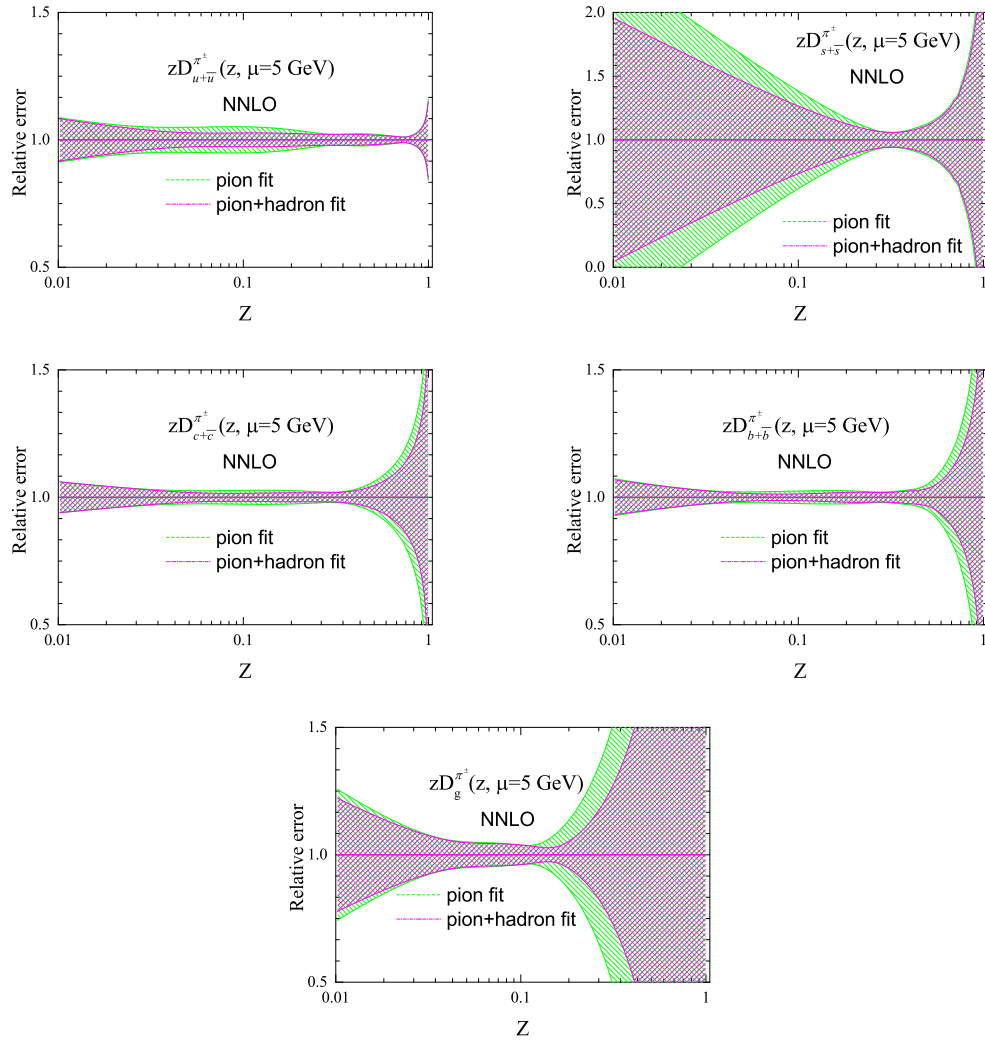


FIG. 2. Same as Fig. 1 but at NNLO.

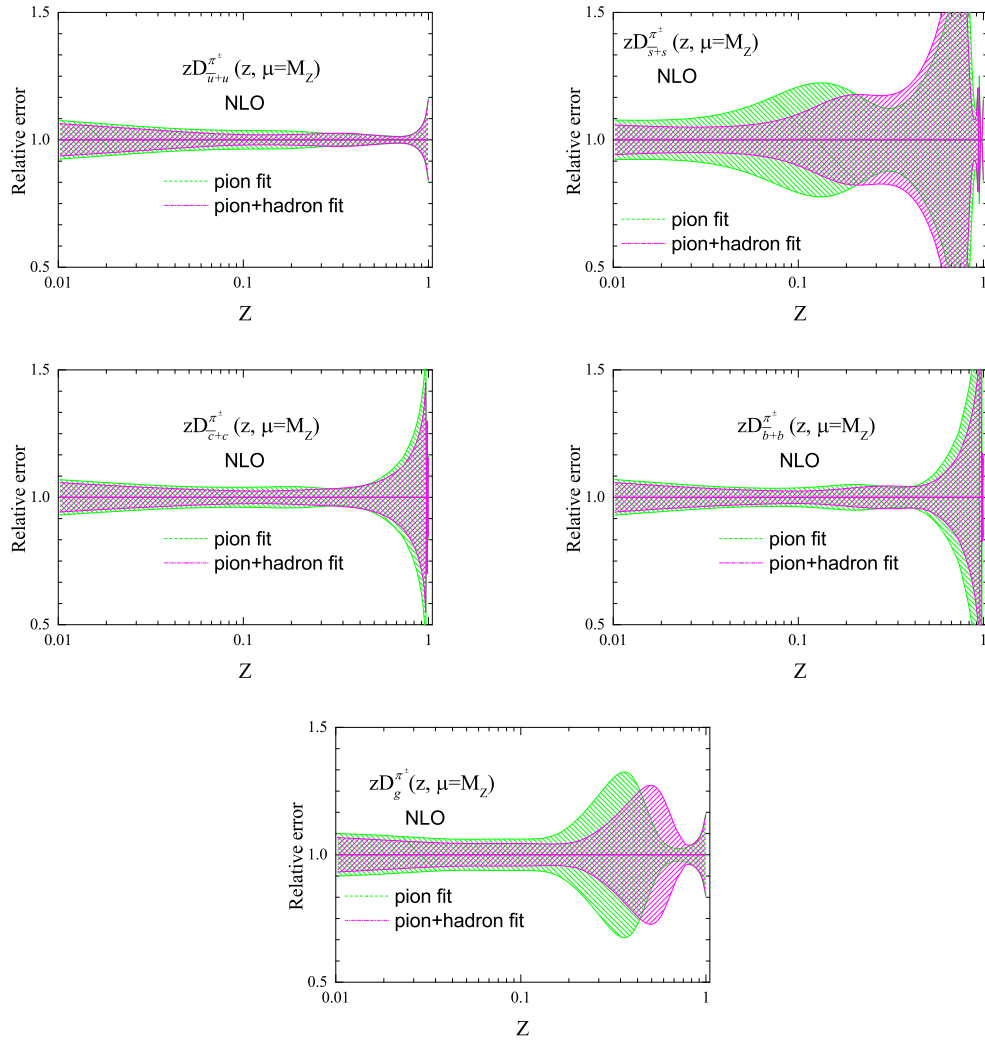


FIG. 3. Same as Fig. 1 but at $Q = M_Z$.

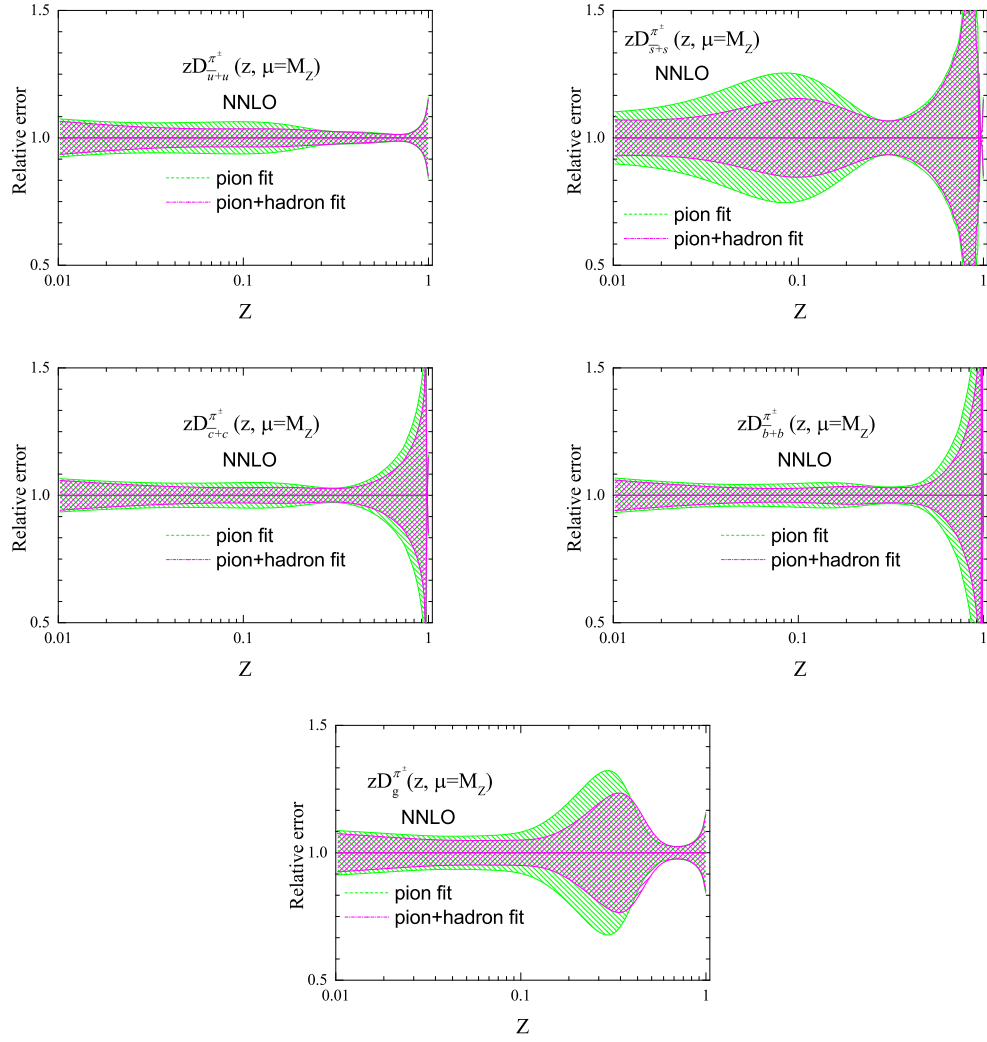


FIG. 4. Same as Fig. 1 but for $Q = M_Z$ at NNLO.

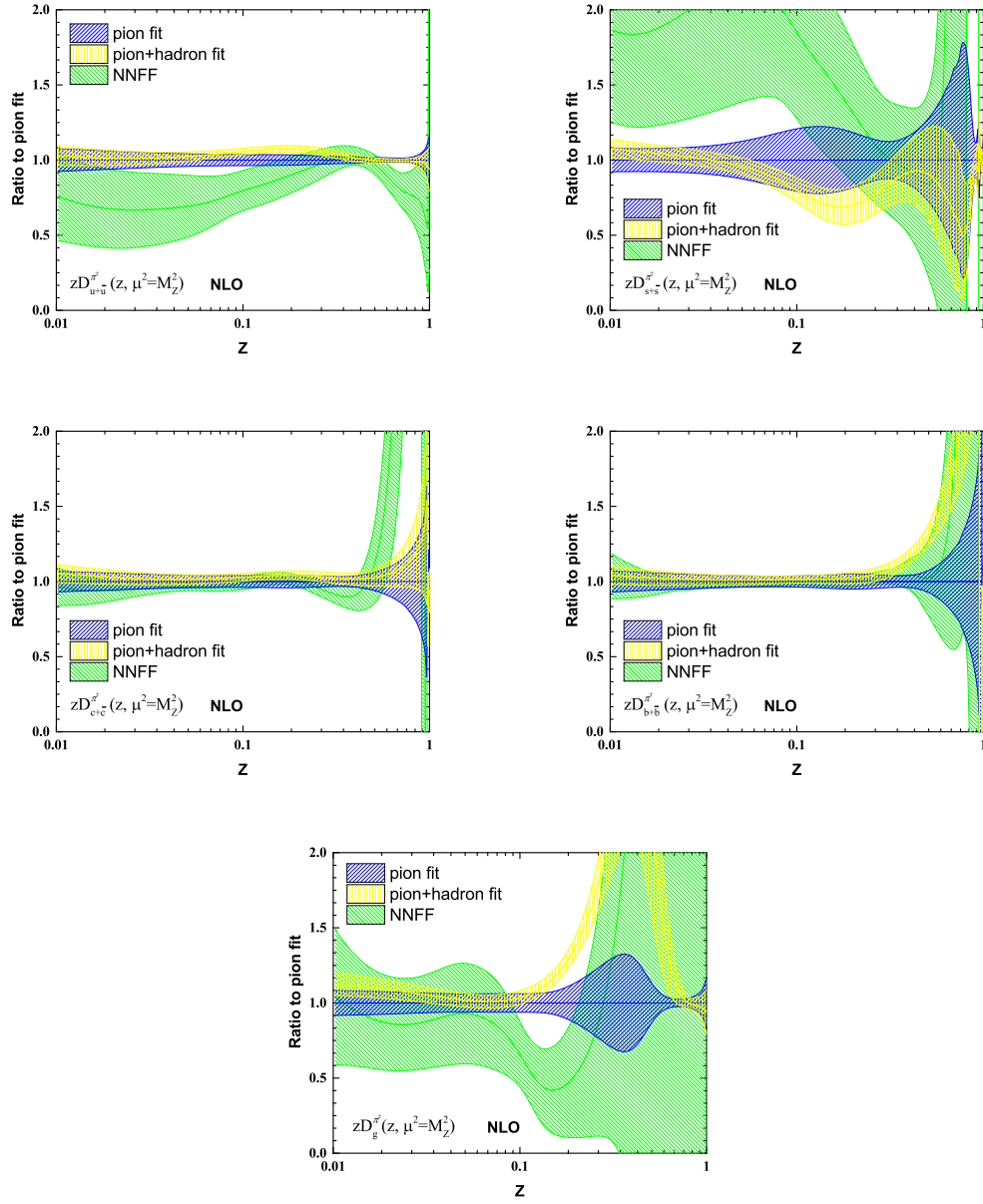


FIG. 5. Comparison between the pion FFs ratios from the “pion fit”, “pion+hadron fit” and NNFF1.0 analyses to the pion FFs from “pion” analysis at NLO for $Q = M_Z$.

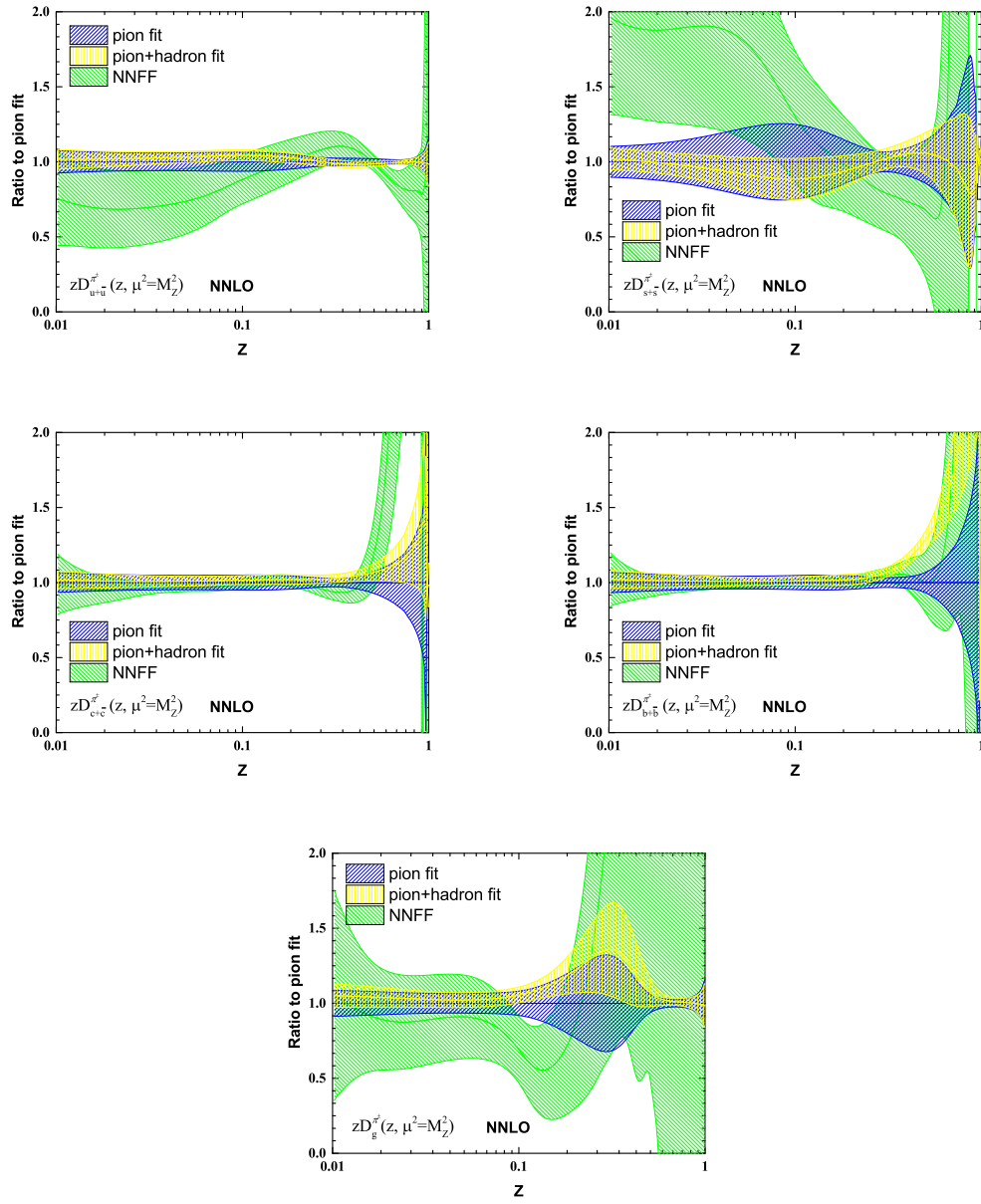


FIG. 6. Same as Fig. 5 but at NNLO.

energy, we recalculate the predictions of Figs. 1 and 2, but this time for $Q = M_z$. The results obtained have been shown in Figs. 3 and 4 at NLO and NNLO, respectively. The reduction in the relative uncertainty of all flavors after the inclusion of the unidentified light charged hadron data in the analysis is clearly seen from these figures. Note that the shift observed in the relative uncertainty of $s + \bar{s}$ and gluon FFs from “pion+hadron fit” analysis compared with the “pion fit” analysis at NLO (see Fig. 3) is due to the considerable change in the central values of these distributions after the inclusion of the hadron data.

Another way for comparing the results of two aforementioned analyses is using the ratio plots in which any change in the central values of the distribution can be also investigated, in addition to their uncertainties. Fig. 5 shows a comparison between the ratios of pion FFs obtained from the “pion+hadron fit” analysis (yellow band) and also NNFF1.0 [9] (green band) to those obtained from the “pion fit” analysis (blue band) at $Q = M_z$ and NLO. According to the results obtained, one can see that the uncertainties of all flavor distributions have been decreased by inclusion the unidentified light charged hadron data in the analysis compared with the “pion fit” analysis. Overall, our FFs whether from the “pion fit” analysis or “pion+hadron fit” one, have less uncertainties than the NNFF1.0 results, especially for the case of up, strange and gluon distributions.

Let us focus on each flavor separately to discuss about the changes in more details. For the case of $u + \bar{u}$ FF, no significant change can be seen between the “pion fit” and “pion+hadron fit” analyses. However, both of these analyses have different results than the $u + \bar{u}$ FF of NNFF1.0, almost for all values of z . Actually, the difference is more significant at lower values of z and reaches even to 30%. The second panel of Fig. 5 shows that the inclusion of hadron data in the analysis of pion FFs at NLO can put further constraints on $s + \bar{s}$ FF, especially at medium to small z regions, so that the uncertainty is remarkably reduced. Moreover, it decreases the $s + \bar{s}$ distribution in magnitude at medium and large values of z . It should be noted that our results for the $s + \bar{s}$ FF are very different to NNFF1.0

result and have smaller magnitude up to 100% at smaller z values. For the case of $c + \bar{c}$ and $b + \bar{b}$ FFs, all three analyses have almost same results both in magnitude and uncertainties at medium to small values of z , but differ at larger values. To be more precise, the $c + \bar{c}$ FF of “pion fit” and “pion+hadron fit” analyses are similar even at large values of z , but the NNFF1.0 result is grows rapidly in this region. In contrast, the $b + \bar{b}$ FF of “pion+hadron fit” analysis behaves more similar to the NNFF1.0 and grows rapidly at large z values compared with the “pion fit” analysis. Overall, one can conclude that the inclusion of the hadron data in the analysis does not affect the $c + \bar{c}$ FF, but can change the $b + \bar{b}$ FF at large values of z . The last panel of Fig. 5 shown again the immense impact of the unidentified light charged hadron data on the gluon FF of pion, especially at medium values of z . As can be seen, in addition to the significant reduction of the gluon FF uncertainty, its central value has changed considerably at around $z = 0.4$ and become more consistent with the NNFF1.0 result at this region. However, there are still some differences at $0.1 \lesssim z \lesssim 0.8$, though all three analyses have almost same results at small z values. Another important point should be noted is the very less uncertainty of our results compared with the NNFF1.0 one, in particular at large z regions which can be attributed to the low flexibility of our parameterization for the gluon FF.

Fig. 6 shows the same results as Fig. 5, but at NNLO accuracy. Overall, the interpretation of results obtained for each flavor distribution is similar to NLO case, with the difference that now the discrepancy observed between the $s + \bar{s}$ and also gluon FFs from “pion fit” and “pion+hadron fit” analyses at medium z regions is more moderate than before. For example, the difference between the gluon FFs obtained from these two analyses at $z \approx 0.4$ is less than 50% according to the last panel of Fig. 6, while it is more than 100% at NLO (see Fig. 5). Another point should be noted is that the $u + \bar{u}$ and $c + \bar{c}$ FFs remain still unchanged after the inclusion of the unidentified light charged hadron data in the analysis, and the $b + \bar{b}$ FF is rapidly grown at large z values just similar to NLO case.

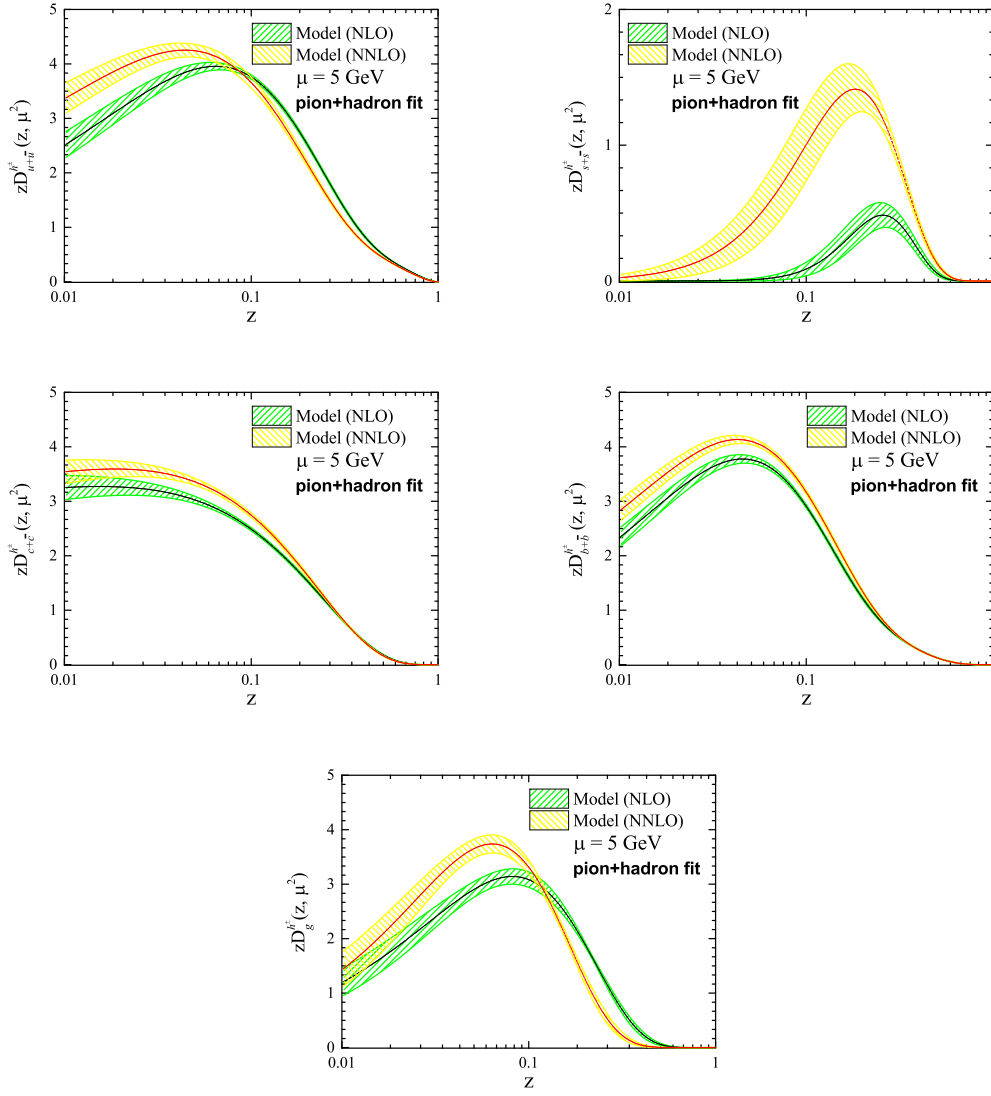


FIG. 7. Comparison between the NLO and NNLO pion FFs determined from a simultaneous analysis of pion and unidentified light charged hadron data, “pion+hadron fit”, for all flavor distributions at $Q_0 = 5$ GeV.

C. Comparison of the “pion+hadron fit” at NLO and NNLO accuracy

Considering the “pion+hadron fit” analysis as a final and more excellent analysis to determine the pion FFs from SIA data, it is also of interest to compare the distributions obtained at NLO and NNLO accuracy. A comparison between the NLO and NNLO pion FFs determined from a simultaneous analysis of pion and unidentified light charged hadron data for all flavor distributions at $Q_0 = 5 \text{ GeV}$ has been shown in Fig. 7. Overall, we can say that no improvement will be achieved in FF uncertainties by going from NLO to NNLO accuracy. However, there are some crucial changes in the central values of the obtained densities. As can be seen, the $u + \bar{u}$ and gluon FFs follow similar manner. To be more precise, although the size of the changes is not too large, but both of them are increased at smaller values of z and decreased at larger values since the NNLO corrections are included. The $c + \bar{c}$ and $b + \bar{b}$ FFs are partially changed just at smaller values of z . But the situation is completely different for the case of $s + \bar{s}$ FF. Actually, the magnitude of its distribution grows to a great extent by considering the NNLO corrections. Note that, although the uncertainty band of $s + \bar{s}$ FF at NNLO is bigger than NLO one, but the relative uncertainties of two distributions (similar to Fig. 1) are of the same order.

D. Comparison of the data and theory predictions

Now we are in a position to complete our study of the fit quality as well as the data vs. theory comparisons.

Here we will focus on the theory prediction based on the extracted pion FFs from our “pion+hadron fit” analysis. We turn to consider only the NNLO results to calculate the normalized cross section for the total, light, c -tagged and b -tagged. To begin with, in Fig. 8, we show the detailed comparisons of $\frac{1}{\sigma_{tot}} \frac{d\sigma^{\pi^\pm}}{dz}$ with the SIA data sets analyzed in this study. These data sets include the charged pion productions at ALEPH, DELPHI, SLD and OPAL experiments. As we can see from this comparison, the agreement between the analyzed

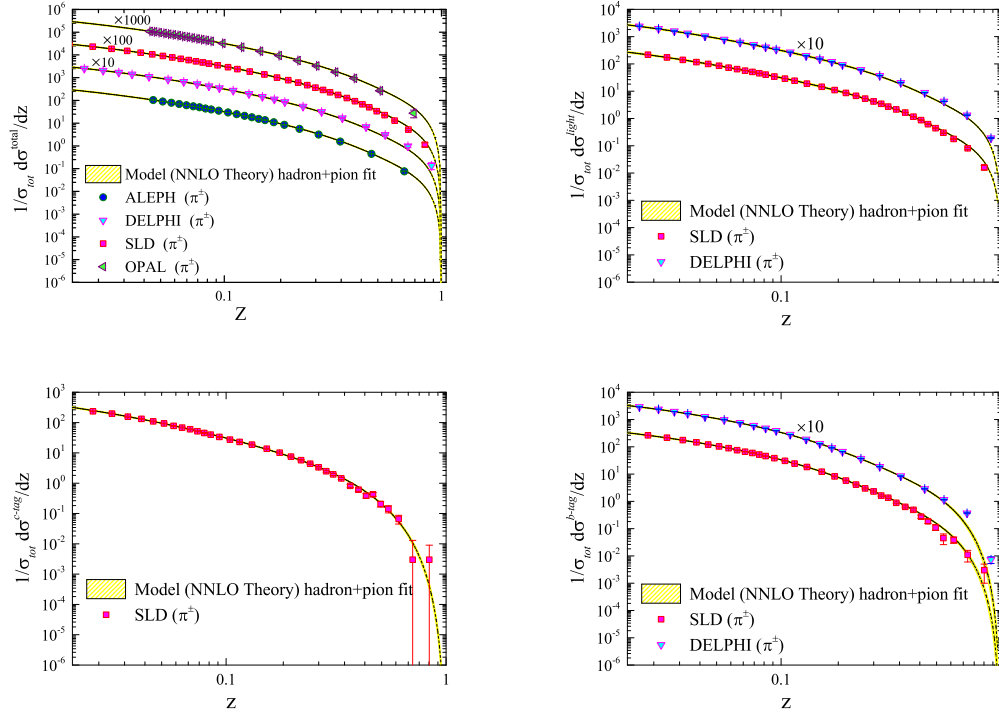


FIG. 8. Detailed comparisons of $\frac{1}{\sigma_{tot}} \frac{d\sigma^{\pi^\pm}}{dz}$ with the SIA data sets for the charged pion productions at ALEPH, DELPHI, SLD and OPAL experiments.

data sets and theoretical predictions for wide range of z are excellent, which show both the validity and the quality of the QCD fits. In Fig. 9, we show the comparison between the NNLO theory based on our “pion+hadron fit” with the charged pion productions at BABAR and BELLE experiments. From the comparisons in this figure, we can see again that the data vs. theory comparisons are excellent.

As a short summary, considering the impact of these two types of data on the pion FFs, shown in plots presented in this section, one sees that in the case of “pion+hadron

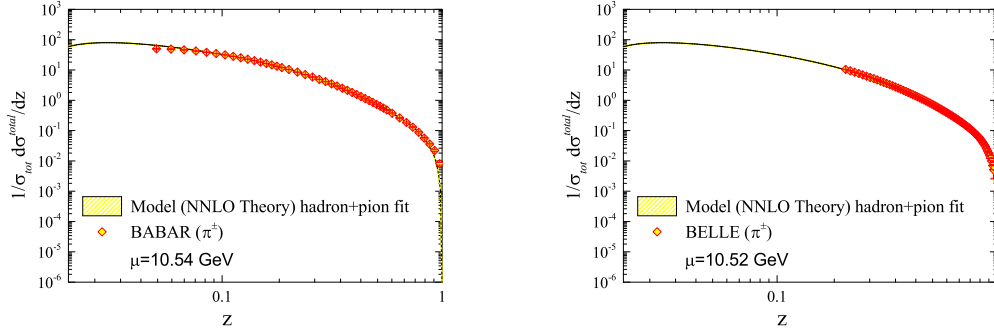


FIG. 9. Detailed comparisons of $\frac{1}{\sigma_{tot}} \frac{d\sigma^{\pi^\pm}}{dz}$ with the SIA data sets for the charged pion productions at BABAR and BELLE experiments.

fit” analysis there is a visible reduction on the pion FFs uncertainties at wide range of z , showing that the inclusion of two data sets simultaneously is somewhat more constraining.

V. SUMMARY AND CONCLUSIONS

In this study, we have quantified the constraints that the unidentified light charged hadron data sets could impose on the determination of pion FFs. To achieve this goal, new determinations of pion FFs at NLO and NNLO QCD corrections have been carried out based on a comprehensive data sets of SIA processes. In this respect, we calculate the pion FFs from QCD analyses of two different data sets. Firstly, the pion FFs are determined through QCD analyses of pion experimental data sets alone, which is referred to as “pion fit”. In addition to the determination of pion FFs using pion experimental data sets, one may certainly expects further constraints to become available for pion FFs studies and an improved knowledge of the FFs will become possible from other source of experimental information. Although the data sets of pion production in electron-positron annihilation

include inclusive, uds -tagged, c -tagged and b -tagged observables, some of the parameters of pion FFs at initial scale can not be constrained well enough. Since the most contribution of unidentified light charged hadrons cross sections in SIA measurements is related to the identified pion production, one can expect further constraints by adding these data sets into the QCD fits. Hence, to achieve the first and new determination of pion FFs, we have explicitly chosen our input dataset and calculated pion FFs adding simultaneously the pion and unidentified light charged hadron data sets in our analysis, which is entitled as “pion+hadron fit”. Our main finding is that using the pion experimental data along with the unidentified light charged hadron data sets has the potential to significantly reduce the pion FFs uncertainties in a wide kinematic range of momentum fraction z .

According to the plots presented in this study, one can clearly see the reduction of pion FFs uncertainties in almost all range of z . The most effects of adding unidentified light charged hadron data sets in “pion+hadron fit” analysis are seen for the $s + \bar{s}$ and gluon FFs. Not only the uncertainties of $s + \bar{s}$ and gluon decrease, but also the behavior of their central values have changed considerably. Consequently, our study shows that applying unidentified light charged hadron observables together with pion production data sets in a calculation of pion FFs leads to somewhat a better fit quality. Since the higher-order corrections are significant, we plan to study the effect arising from higher order correction in the determination of pion FFs. Since we include the SIA data sets in our analyses, the perturbative QCD corrections up to NNLO accuracy can be considered. We found that our results at NNLO corrections improved the fit quality in comparison to the NLO accuracy and it leads to reduction of the χ^2 for all data sets separately as well as for the total χ^2 . By considering the NNLO corrections, similar slight improvements in the FFs uncertainty are also found in some region of z .

The two analyses presented in this study share, however, a common limitation. In both cases, it has indeed been necessary to include other source of experimental information such as the data from semi-inclusive deep inelastic scattering (SIDIS), and proton-proton

and proton-antiproton collisions measured by TEVATRON, RHIC and LHC. However, the NNLO calculations for such processes are not yet available, which would require a relentless effort for the QCD calculations. It is worth mentioning here that our investigations in this study could be extended to the new determination of kaon and proton FFs considering the unidentified light charged hadron data sets as well as the identified charged hadron production observables. More detailed discussions of these new determination of kaon and proton FFs will be presented in our upcoming study.

ACKNOWLEDGMENTS

Authors are thankful to Valerio Bertone for many helpful discussions and comments. Authors thank School of Particles and Accelerators, Institute for Research in Fundamental Sciences (IPM) for financial support of this project. Hamzeh Khanpour also is thankful the University of Science and Technology of Mazandaran for financial support provided for this research.

-
- [1] R. A. Khalek, S. Bailey, J. Gao, L. Harland-Lang and J. Rojo, "Towards Ultimate Parton Distributions at the High-Luminosity LHC," *Eur. Phys. J. C* **78**, no. 11, 962 (2018), [arXiv:1810.03639 [hep-ph]].
 - [2] J. Gao, L. Harland-Lang and J. Rojo, "The Structure of the Proton in the LHC Precision Era," *Phys. Rept.* **742**, 1 (2018), [arXiv:1709.04922 [hep-ph]].
 - [3] J. Rojo *et al.*, "The PDF4LHC report on PDFs and LHC data: Results from Run I and preparation for Run II," *J. Phys. G* **42**, 103103 (2015), [arXiv:1507.00556 [hep-ph]].
 - [4] S. Forte and G. Watt, "Progress in the Determination of the Partonic Structure of the Proton," *Ann. Rev. Nucl. Part. Sci.* **63**, 291 (2013) doi:10.1146/annurev-nucl-102212-170607 [arXiv:1301.6754 [hep-ph]].
 - [5] R. D. Ball and A. Deshpande, "The proton spin, semi-inclusive processes, and measurements at a future Electron Ion Collider," arXiv:1801.04842 [hep-ph].

- [6] R. D. Ball *et al.* [NNPDF Collaboration], “Parton distributions from high-precision collider data,” *Eur. Phys. J. C* **77**, no. 10, 663 (2017), [arXiv:1706.00428 [hep-ph]].
- [7] S. Alekhin, J. Blumlein, S. Moch and R. Placakyte, “Parton distribution functions, α_s , and heavy-quark masses for LHC Run II,” *Phys. Rev. D* **96**, no. 1, 014011 (2017), [arXiv:1701.05838 [hep-ph]].
- [8] V. Bertone *et al.* [NNPDF Collaboration], “Charged hadron fragmentation functions from collider data,” *Eur. Phys. J. C* **78**, no. 8, 651 (2018), [arXiv:1807.03310 [hep-ph]].
- [9] V. Bertone *et al.* [NNPDF Collaboration], “A determination of the fragmentation functions of pions, kaons, and protons with faithful uncertainties,” *Eur. Phys. J. C* **77**, no. 8, 516 (2017), [arXiv:1706.07049 [hep-ph]].
- [10] M. Soleymaninia, H. Khanpour and S. M. Moosavi Nejad, “First determination of D^{*+} -meson fragmentation functions and their uncertainties at next-to-next-to-leading order,” *Phys. Rev. D* **97**, no. 7, 074014 (2018) [arXiv:1711.11344 [hep-ph]].
- [11] M. Soleymaninia, M. Goharipour and H. Khanpour, “First QCD analysis of charged hadron fragmentation functions and their uncertainties at next-to-next-to-leading order,” *Phys. Rev. D* **98**, no. 7, 074002 (2018) [arXiv:1805.04847 [hep-ph]].
- [12] A. Mohamaditabar, F. Taghavi-Shahri, H. Khanpour and M. Soleymaninia, “Determination of contributions from residual light charged hadrons to inclusive charged hadrons from e^+e^- annihilation data,” arXiv:1808.09255 [hep-ph].
- [13] M. Hirai, H. Kawamura, S. Kumano and K. Saito, “Impacts of B-factory measurements on determination of fragmentation functions from electron-positron annihilation data,” *PTEP* **2016**, no. 11, 113B04 (2016), [arXiv:1608.04067 [hep-ph]].
- [14] S. M. Moosavi Nejad, M. Soleymaninia and A. Maktoubian, “Proton fragmentation functions considering finite-mass corrections,” *Eur. Phys. J. A* **52**, no. 10, 316 (2016), [arXiv:1512.01855 [hep-ph]].
- [15] S. M. Moosavi Nejad and P. Sartipi Yarahmadi, “Heavy quark fragmentation functions at next-to-leading perturbative QCD,” *Eur. Phys. J. A* **52**, no. 10, 315 (2016) [arXiv:1609.07422 [hep-ph]].
- [16] S. M. Moosavi Nejad, “NLO QCD corrections to triply heavy baryon fragmentation function considering the effect of nonperturbative dynamics of baryon bound states,” *Phys. Rev. D* **96**, no. 11, 114021 (2017).

- [17] M. Soleymaninia, A. N. Khorramian, S. M. Moosavi Nejad and F. Arbabifar, "Determination of pion and kaon fragmentation functions including spin asymmetries data in a global analysis," Phys. Rev. D **88**, no. 5, 054019 (2013) Addendum: [Phys. Rev. D **89**, no. 3, 039901 (2014)], [arXiv:1306.1612 [hep-ph]].
- [18] G. R. Boroun, S. Zarrin and S. Dadfar, "Laplace method for the evolution of the fragmentation function of B_c mesons," Nucl. Phys. A **953**, 21 (2016).
- [19] G. R. Boroun, T. Osati and S. Zarrin, "An Approximation Approach to the Evolution of the Fragmentation Function," Int. J. Theor. Phys. **54**, no. 10, 3831 (2015).
- [20] M. Zarei, F. Taghavi-Shahri, S. Atashbar Tehrani and M. Sarbishei, "Fragmentation functions of the pion, kaon, and proton in the NLO approximation: Laplace transform approach," Phys. Rev. D **92**, no. 7, 074046 (2015), [arXiv:1601.02815 [hep-ph]].
- [21] D. de Florian *et al.* [LHC Higgs Cross Section Working Group], "Handbook of LHC Higgs Cross Sections: 4. Deciphering the Nature of the Higgs Sector," arXiv:1610.07922 [hep-ph].
- [22] S. Alioli, M. Farina, D. Pappadopulo and J. T. Ruderman, "Precision Probes of QCD at High Energies," JHEP **1707**, 097 (2017), [arXiv:1706.03068 [hep-ph]].
- [23] R. D. Ball *et al.* [NNPDF Collaboration], "Precision determination of the strong coupling constant within a global PDF analysis," Eur. Phys. J. C **78**, no. 5, 408 (2018), [arXiv:1802.03398 [hep-ph]].
- [24] V. N. Gribov and L. N. Lipatov, "Deep inelastic e p scattering in perturbation theory," Sov. J. Nucl. Phys. **15**, 438 (1972) [Yad. Fiz. **15**, 781 (1972)].
- [25] L. N. Lipatov, "The parton model and perturbation theory," Sov. J. Nucl. Phys. **20**, 94 (1975) [Yad. Fiz. **20**, 181 (1974)].
- [26] G. Altarelli and G. Parisi, "Asymptotic Freedom in Parton Language," Nucl. Phys. B **126**, 298 (1977).
- [27] Y. L. Dokshitzer, "Calculation of the Structure Functions for Deep Inelastic Scattering and e^+e^- Annihilation by Perturbation Theory in Quantum Chromodynamics.," Sov. Phys. JETP **46**, 641 (1977) [Zh. Eksp. Teor. Fiz. **73**, 1216 (1977)].
- [28] N. Sato, J. J. Ethier, W. Melnitchouk, M. Hirai, S. Kumano and A. Accardi, "First Monte Carlo analysis of fragmentation functions from single-inclusive e^+e^- annihilation," Phys. Rev. D **94**, no. 11, 114004 (2016), [arXiv:1609.00899 [hep-ph]].
- [29] S. Albino, B. A. Kniehl and G. Kramer, "Fragmentation functions for $K_0(S)$ and Lambda with

- complete quark flavor separation,” Nucl. Phys. B **734**, 50 (2006), [hep-ph/0510173].
- [30] S. Albino, B. A. Kniehl and G. Kramer, “AKK Update: Improvements from New Theoretical Input and Experimental Data,” Nucl. Phys. B **803**, 42 (2008), [arXiv:0803.2768 [hep-ph]].
- [31] C. A. Aidala, F. Ellinghaus, R. Sassot, J. P. Seele and M. Stratmann, “Global Analysis of Fragmentation Functions for Eta Mesons,” Phys. Rev. D **83**, 034002 (2011), [arXiv:1009.6145 [hep-ph]].
- [32] S. Kretzer, “Fragmentation functions from flavor inclusive and flavor tagged e^+e^- annihilations,” Phys. Rev. D **62**, 054001 (2000), [hep-ph/0003177].
- [33] B. A. Kniehl, G. Kramer and B. Potter, “Fragmentation functions for pions, kaons, and protons at next-to-leading order,” Nucl. Phys. B **582**, 514 (2000), [hep-ph/0010289].
- [34] D. P. Anderle, T. Kaufmann, M. Stratmann, F. Ringer and I. Vitev, “Using hadron-in-jet data in a global analysis of D^* fragmentation functions,” Phys. Rev. D **96**, no. 3, 034028 (2017), [arXiv:1706.09857 [hep-ph]].
- [35] L. Bourhis, M. Fontannaz, J. P. Guillet and M. Werlen, “Next-to-leading order determination of fragmentation functions,” Eur. Phys. J. C **19**, 89 (2001), [hep-ph/0009101].
- [36] D. de Florian, R. Sassot and M. Stratmann, “Global analysis of fragmentation functions for protons and charged hadrons,” Phys. Rev. D **76**, 074033 (2007), [arXiv:0707.1506 [hep-ph]].
- [37] M. Leitgab *et al.* [Belle Collaboration], “Precision Measurement of Charged Pion and Kaon Differential Cross Sections in e^+e^- Annihilation at $\sqrt{s}=10.52\text{ GeV}$,” Phys. Rev. Lett. **111**, 062002 (2013) [arXiv:1301.6183 [hep-ex]].
- [38] J. P. Lees *et al.* [BaBar Collaboration], “Production of charged pions, kaons, and protons in e^+e^- annihilations into hadrons at $\sqrt{s}=10.54\text{ GeV}$,” Phys. Rev. D **88**, 032011 (2013) [arXiv:1306.2895 [hep-ex]].
- [39] R. Brandelik *et al.* [TASSO Collaboration], “Charged Pion, Kaon, Proton and anti-Proton Production in High-Energy e^+e^- Annihilation,” Phys. Lett. **94B**, 444 (1980).
- [40] M. Althoff *et al.* [TASSO Collaboration], “Charged Hadron Composition of the Final State in e^+e^- Annihilation at High-Energies,” Z. Phys. C **17**, 5 (1983).
- [41] H. Aihara *et al.* [TPC/Two Gamma Collaboration], “Charged hadron inclusive cross-sections and fractions in e^+e^- annihilation $\sqrt{s} = 29\text{ GeV}$,” Phys. Rev. Lett. **61**, 1263 (1988).
- [42] W. Braunschweig *et al.* [TASSO Collaboration], “Pion, Kaon and Proton Cross-sections in e^+e^- Annihilation at 34-GeV and 44-GeV Center-of-mass Energy,” Z. Phys. C **42**, 189 (1989).

- [43] D. Buskulic *et al.* [ALEPH Collaboration], “Inclusive π^{+-} , K^{+-} and (p, anti-p) differential cross-sections at the Z resonance,” *Z. Phys. C* **66**, 355 (1995).
- [44] P. Abreu *et al.* [DELPHI Collaboration], “ π^{+-} , K^{+-} , p and anti-p production in $Z^0 \rightarrow q \text{ anti-}q$, $Z^0 \rightarrow c \text{ anti-}c$, $Z^0 \rightarrow b \text{ anti-}b$, $Z^0 \rightarrow u \text{ anti-}u$, d anti-d, s anti-s,” *Eur. Phys. J. C* **5**, 585 (1998).
- [45] R. Akers *et al.* [OPAL Collaboration], “Measurement of the production rates of charged hadrons in $e^+ e^-$ annihilation at the Z^0 ,” *Z. Phys. C* **63**, 181 (1994).
- [46] K. Abe *et al.* [SLD Collaboration], “Production of π^+ , π^- , K^+ , K^- , p and anti-p in light (uds), c and b jets from Z^0 decays,” *Phys. Rev. D* **69**, 072003 (2004) [hep-ex/0310017].
- [47] W. Braunschweig *et al.* [TASSO Collaboration], “Global Jet Properties at 14-GeV to 44-GeV Center-of-mass Energy in $e^+ e^-$ Annihilation,” *Z. Phys. C* **47**, 187 (1990).
- [48] D. Buskulic *et al.* [ALEPH Collaboration], “Measurement of α_s from scaling violations in fragmentation functions in $e^+ e^-$ annihilation,” *Phys. Lett. B* **357**, 487 (1995) Erratum: [*Phys. Lett. B* **364**, 247 (1995)].
- [49] P. Abreu *et al.* [DELPHI Collaboration], “Measurement of the quark and gluon fragmentation functions in Z^0 hadronic decays,” *Eur. Phys. J. C* **6**, 19 (1999).
- [50] K. Ackerstaff *et al.* [OPAL Collaboration], “Measurements of flavor dependent fragmentation functions in $Z^0 \rightarrow q \text{ anti-}q$ events,” *Eur. Phys. J. C* **7**, 369 (1999), [hep-ex/9807004].
- [51] R. Akers *et al.* [OPAL Collaboration], “Measurement of the longitudinal, transverse and asymmetry fragmentation functions at LEP,” *Z. Phys. C* **68**, 203 (1995).
- [52] P. J. Rijken and W. L. van Neerven, “Higher order QCD corrections to the transverse and longitudinal fragmentation functions in electron - positron annihilation,” *Nucl. Phys. B* **487**, 233 (1997), [hep-ph/9609377].
- [53] A. Mitov and S. O. Moch, “QCD Corrections to Semi-Inclusive Hadron Production in Electron-Positron Annihilation at Two Loops,” *Nucl. Phys. B* **751**, 18 (2006), [hep-ph/0604160].
- [54] P. J. Rijken and W. L. van Neerven, “ $\mathcal{O}(\alpha_s^2)$ contributions to the longitudinal fragmentation function in $e^+ e^-$ annihilation,” *Phys. Lett. B* **386**, 422 (1996), [hep-ph/9604436].
- [55] V. Bertone, S. Carrazza and J. Rojo, “APFEL: A PDF Evolution Library with QED corrections,” *Comput. Phys. Commun.* **185**, 1647 (2014), [arXiv:1310.1394 [hep-ph]].
- [56] M. Tanabashi *et al.* [Particle Data Group], “Review of Particle Physics,” *Phys. Rev. D* **98**, no. 3, 030001 (2018).
- [57] H. Khanpour and S. Atashbar Tehrani, “Global Analysis of Nuclear Parton Distribution

Functions and Their Uncertainties at Next-to-Next-to-Leading Order," Phys. Rev. D **93**, no. 1, 014026 (2016), [arXiv:1601.00939 [hep-ph]].